Sesquiterpenoids from the Endophytic Fungus *Rhinocladiella similis*

Shuai Liu,[†,‡] Yuping Zhao,[‡] Christian Heering,[§] Christoph Janiak,[§] Werner E. G. Müller,[⊥] Sergi Hervé Akoné,[†,#] Zhen Liu,*[†] and Peter Proksch*[†]

[†]Institute of Pharmaceutical Biology and Biotechnology, Heinrich-Heine-Universität Düsseldorf, 40225 Düsseldorf, Germany
[‡]Faculty of Life Science and Food Engineering, Huaiyin Institute of Technology, Huaian 223003, People's Republic of China
[§]Institute of Inorganic and Structural Chemistry, Heinrich-Heine-Universität Düsseldorf, 40225 Düsseldorf, Germany
[⊥]Institute of Physiological Chemistry, Universitätsmedizin der Johannes Gutenberg-Universität Mainz, 55128 Mainz, Germany
[#]Department of Chemistry, Faculty of Science, University of Douala, PO Box 24157, Douala, Cameroon

S *Supporting Information*

ABSTRACT: Ten new sesquiterpenoid derivatives, rhinomilisins A−J (**1**−**10**), along with six known analogues (**11**−**16**), were isolated from the mangrove-derived endophytic fungus *Rhinocladiella similis*. The structures of the new compounds were elucidated by their NMR and MS data, while the absolute configuration of **3** and **6** was determined by X-ray crystallographic analysis and Mosher's method, respectively. All isolated compounds (**1**−**16**) were evaluated for their cytotoxicity against the mouse lymphoma cell line L5178Y, and compounds **1**, **7**, and **15** showed moderate activity with IC$_{50}$ values of 5.0, 8.7, and 24.4 μM, respectively.

Rhinocladiella similis
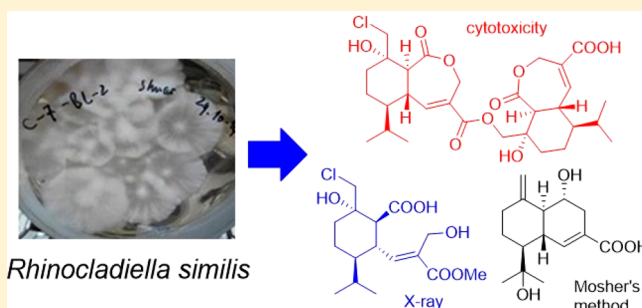
S ince the discovery of penicillin by Alexander Fleming in 1928, many fungal natural products and their derivatives have been used as drugs or drug candidates for the treatment of bacterial, fungal, or parasitic diseases and cancer or as immunosuppressive or cholesterol-lowering agents.[1] During the past decade, fungi from special ecological niches such as mangrove endophytes have attracted considerable attention of scientists due to their production of diverse structurally unique and bioactive secondary metabolites.[2,3] Plinabulin, derived from the marine fungal product halimide, is now in phase III clinical trials as a new type of anticancer drug.[4,5]

As part of our ongoing investigations on endophytic fungi,[6−8] *Rhinocladiella similis* was isolated from the mangrove fern *Acrostichum aureum*. A new dimeric sesquiterpenoid (**1**), four new heptelidic acid derivatives (**2**−**5**), five new cadalene-type sesquiterpenoids (**6**−**10**), and six known compounds including heptelidic acid chlorohydrin (**11**),[9] trichoderonic acid A (**12**),[10] hydroheptelidic acid (**13**),[11] xylaric acid D (**14**),[9] gliocladic acid (**15**),[12] and xylaric acid A (**16**),[9] were isolated from the EtOAc extract of *R. similis* after fermentation on solid rice medium containing sea salt. The structures of the isolated metabolites were determined by analysis of NMR and MS data as well as by comparison with the literature. Heptelidic acid was previously reported as a potent cytotoxic agent against several human tumor cell lines,[13] as a potent inhibitor of glyceraldehyde-3-phosphate dehydrogenase,[14] and as a potent regulator of apoptosis.[15] Heptelidic acid derivatives were discovered previously from several fungi from the class Sordariomycetes including *Xylaria* sp.,[9,16] *Chaetomium globosum*,[12] *Acremonium* sp.,[17] *Gliocladium virens*,[18] and *Thricho-*

derma sp.[10−12] In this study, the discovery of heptelidic acid derivatives from *Rhinocladiella similis*, which belongs to the class Eurotiomycetes, proves this fungus has gene clusters for the biosynthesis of heptelidic acid derivatives.

■ RESULTS AND DISCUSSION

Compound **1** was isolated as a white, amorphous powder. Its molecular formula was determined as C$_{30}$H$_{41}$ClO$_{10}$ by HRESIMS. The ^{1}H NMR data of **1** (Table 1) exhibited two sets of signals that were similar to those of two coisolated known compounds, heptelidic acid chlorohydrin[9] (**11**) and trichoderonic acid A[10] (**12**), suggesting that **1** was a dimer of heptelidic acid derivatives. Compared to the chemical shifts of H$_{ab}$-14 (δ_H 4.82 and 3.92) and C-14 (δ_C 48.1), the downfield-shifted signals of H$_{ab}$-14′ (δ_H 5.21 and 4.56) and C-14′ (δ_C 66.9) suggested that the methylene moiety at C-14′ was oxygenated rather than chlorinated. Detailed analysis of the 2D NMR spectra of **1** established two sesquiterpenoid substructures from C-1 to C-15 and from C-1′ to C-15′ (Figure 1). The HMBC correlations from H$_{ab}$-14′ to the carboxy C-15 (δ_C 166.9) confirmed the 15,14′-ester linkage of the two substructures. Thus, the planar structure of **1** was elucidated as shown and named rhinomilisin A. The relative configuration of **1** was suggested to be identical to that of heptelidic acid chlorohydrin[9] (**11**) and trichoderonic acid A[10] (**12**) based on similar coupling constants and NOE relationships.

Chart 1
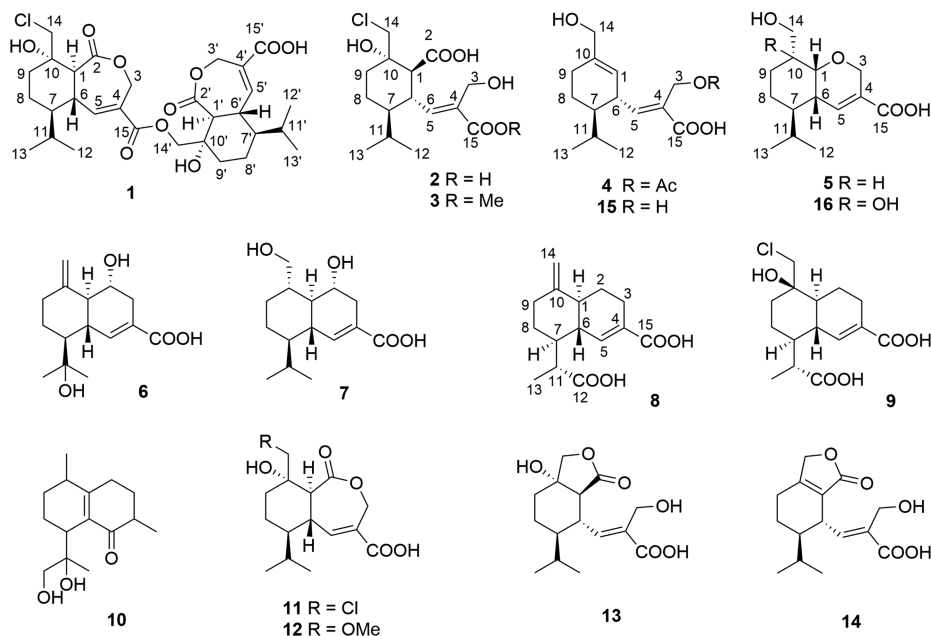
Table 1. ^{1}H and ^{13}C NMR Data of Compound 1^a

position	δ_C, type^b	δ_H (J in Hz)	position	δ_C, type^b	δ_H (J in Hz)
1	54.0, CH	3.74, d (12.6)	1′	54.2, CH	3.62, d (12.6)
2	174.1, C		2′	174.3, C	
3	62.5, CH$_2$	5.28, d (14.7)	3′	62.6, CH$_2$	5.22, d (14.6)
		5.06, d (14.7)			5.05, d (14.6)
4	130.1, C		4′	130.9, C	
5	147.2, CH	7.30, d (4.1)	5′	146.5, CH	7.25, d (4.1)
6	41.3, CH	2.64, m	6′	41.2, CH	2.66, m
7	49.8, CH	1.59, m	7′	49.6, CH	1.58, m
8	22.1, CH$_2$	1.76, m	8′	22.3, CH$_2$	1.73, m
		1.32, m			1.34, m
9	36.1, CH$_2$	2.47, dt (12.9, 3.2)	9′	35.9, CH$_2$	2.19, dt (12.9, 3.2)
		1.38, m			1.44, m
10	74.0, C		10′	73.9, C	
11	28.6, CH	2.16, m	11′	28.7, CH	2.13, m
12	21.7, CH$_3$	1.00, d (6.9)	12′	21.6, CH$_3$	0.99, d (6.9)
13	15.6, CH$_3$	0.94, d (6.9)	13′	15.6, CH$_3$	0.92, d (6.9)
14	48.1, CH$_2$	4.82, d (12.3),	14′	66.9, CH$_2$	5.21, d (12.5)
		3.92, d (12.3)			4.56, d (12.5)
15	166.9, C		15′	168.5, C	

^{a}Recorded at 600 MHz (^{1}H) and 150 MHz (^{13}C) in CD$_3$OD. ^{b}Data were extracted from HSQC and HMBC.

The molecular formula of compound **2** was determined as C$_{15}$H$_{23}$ClO$_6$ with four degrees of unsaturation from the HRESIMS data, containing an additional H$_2$O compared to heptelidic acid chlorohydrin^9 (**11**). The NMR data of **2** (Table 2) resembled those of **11** except for the obvious upfield-shifted H$_2$-3 (δ_H 4.30) and C-3 (δ_C 57.6) in **2**, which indicated cleavage of the 2,3-ester linkage in **2**. Detailed analysis of the 2D NMR spectra of **2** (Figure 1) revealed that the remaining structure of **2** was identical to that of **11**.

Rhinomilisin C (**3**) was obtained as colorless crystals. The molecular formula of **3** was C$_{16}$H$_{25}$ClO$_6$, as deduced from the HRESIMS data. The NMR data of **3** (Table 2) were very similar to those of **2**, except for the appearance of an additional methoxy group (δ_C 52.4 and δ_H 3.75) in **3**. The attachment of this methoxy group at C-15 was supported by the HMBC correlation from the protons of the methoxy group to C-15 (δ_C 169.0). Thus, compound **3** was elucidated as the methyl ester of **2**. The absolute configuration of **3** was further determined as (1S, 6S, 7R, 10S) by X-ray crystallographic analysis (Figure 2).

Based on the HRESIMS data, the molecular formula of **4** was determined as C$_{16}$H$_{24}$O$_5$. The ^{1}H NMR data of **4** (Table 2) were almost identical to those of the coisolated known compound glioclacic acid^{12} (**15**). The obvious difference was the appearance of an additional methyl group (δ_C 20.5 and δ_H 2.03, s) and an additional carboxy group (δ_C 172.2) in **4**. The downfield shift of H$_2$-3 (δ_H 4.86) and C-3 (δ_C 59.3) as well as the HMBC correlations from the additional methyl group and
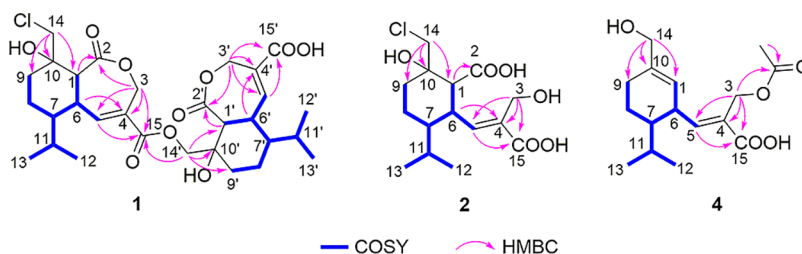

Figure 1. COSY and key HMBC correlations of **1**, **2**, and **4**.

Table 2. ^{1}H and ^{13}C NMR Data of Compounds 2−4

position	δ_C, type (2^a)	δ_H (J in Hz) (2^a)	δ_C, type (3^a)	δ_H (J in Hz) (3^a)	δ_C, type (4^b)	δ_H (J in Hz) (4^b)
1	60.3, CH	2.65, d (11.7)	60.2, CH	2.65, d (11.7)	122.8, CH	5.27, br s
2	176.0, C		175.9, C			
3	57.6, CH$_2$	4.30, s	57.4, CH$_2$	4.31, s	59.3, CH$_2$	4.86, s
4	134.8, C		134.6, C		129.0, C	
5	146.5, CH	6.50, d (10.7)	146.6, CH	6.48, d (10.7)	153.4, CH	6.75, d (10.8)
6	41.9, CH	2.84, q (11.0)	41.9, CH	2.84, q (11.0)	40.3, CH	3.21, m
7	47.8, CH	1.38, m	47.8, CH	1.38, m	46.4, CH	1.36, m
8	21.4, CH$_2$	1.68, m	21.4, CH$_2$	1.67, m	22.1, CH$_2$	1.81, m
		1.20, m		1.19, m		1.36, m
9	35.9, CH$_2$	2.44, dt (12.9, 3.0)	35.9, CH$_2$	2.44, dt (12.9, 3.1)	26.5, CH$_2$	2.13, m
		1.36, m		1.36, m		2.04, m
10	73.3, C		73.3, C		141.3, C	
11	29.5, CH	1.72, m	29.5, CH	1.69, m	29.7, CH	1.67, m
12	21.9, CH$_3$	0.94, d (7.0)	21.9, CH$_3$	0.93, d (7.0)	21.4, CH$_3$	0.97, d (6.9)
13	16.1, CH$_3$	0.81, d (6.8)	16.0, CH$_3$	0.80, d (6.8)	16.9, CH$_3$	0.83, d (6.9)
14	49.2, CH$_2$	3.99, d (12.3)	49.1, CH$_2$	3.99, d (12.3)	66.5, CH$_2$	3.95, d (13.3)
		3.91, d (12.3)		3.90, d (12.3)		3.92, d (13.3)
15	170.2, C		169.0, C		169.9, C	
OMe			52.4, CH$_3$	3.75, s		
OAc					172.2, C	
					20.5, CH$_3$	2.03, s

^{a}Recorded at 300 MHz (^{1}H) and 75 MHz (^{13}C) in CD$_3$OD. ^{b}Recorded at 700 MHz (^{1}H) and 175 MHz (^{13}C) in CD$_3$OD.
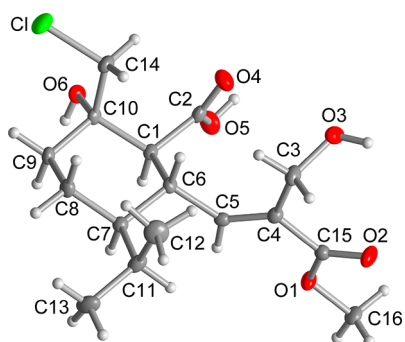

Figure 2. Molecular structure of **3** from a single-crystal X-ray structure determination.

H$_2$-3 to the additional carboxy group indicated the presence of an acetoxy group at C-3 in **4** (Figure 1).

Compound **5** was isolated as a colorless oil. Its molecular formula was determined as C$_{14}$H$_{22}$O$_4$, containing one less oxygen atom compared to the coisolated known compound xylaric acid A (**16**).^{9} By comparing the ^{1}H and ^{13}C NMR data of **5** (Table 3) with those of **16**, it was found that the oxygenated carbon (C-10) in **16** was replaced by a methine group (δ_H 1.65 and δ_C 44.6, CH-10) in **5**. The COSY correlations between H-10/H-1 (δ_H 3.69), H-10/H$_b$-9 (δ_H 1.30), and H-10/H$_{ab}$-14 (δ_H 3.67 and 3.47) together with the HMBC correlations from H$_{ab}$-14 to C-1 (δ_C 73.7), C-9 (δ_C 24.6), and C-10 (δ_C 44.6) confirmed **5** to be the 10-dehydroxy derivative of **16** (Figure 3). The small coupling constants between H-1/H-6 and H-1/H-10 (2.2 Hz) as well as the NOE correlations between H-10/H-1, H-1/H-6 (δ_H 2.01), and H-6/Me-13 (δ_H 0.90) indicated these protons were on the same face of the ring. Thus, the structure of **5** was elucidated as shown.

Rhinomilisin F (**6**) was obtained as white, amorphous powder. The molecular formula of **6** was determined as C$_{15}$H$_{22}$O$_4$ by HRESIMS, indicating five degrees of unsaturation. The ^{1}H NMR spectrum of **6** showed an olefinic proton at δ_H 7.85 (H-5), an exocyclic olefin at δ_H 4.94 and 4.87 (H$_{ab}$-14), an oxygenated methine at δ_H 3.95 (H-2), three aliphatic methines, three aliphatic methylenes, and two methyl groups at δ_H 1.23 and 1.18 (Me-12 and 13) (Table 3). The COSY correlations between H$_{ab}$-9/H$_{ab}$-8/H-7/H-6/H-1/H-2/H$_{ab}$-3 and between H-5/H-6 along with the HMBC correlations from H-3a (δ_H 2.80) and H-5 to C-15 (δ_C 171.1), from Me-12 and Me-13 to C-7 (δ_C 53.9) and C-11 (δ_C 74.2), and from H$_{ab}$-14 to C-9 (δ_C 38.1), C-1 (δ_C 52.2), and C-10 (δ_C 149.8) established the planar structure of **6** as shown, representing a new cadalene-type sesquiterpenoid derivative (Figure 3). The large coupling constants between H-1/H-2 and H-1/H-6 (10.0 Hz) as well as the NOE correlations between H-1 (δ_H 1.97)/H-7 (δ_H 1.64) indicated that H-1 and H-7 were on the same face of the ring, while H-2 and H-6 were on the opposite face. Furthermore, Mosher's method was applied to determine the absolute configuration of C-2 as *R* (Figure 4). Thus, the absolute configurations at C-1, C-6, and C-7 were assigned as 1*S*, 6*S*, and 7*S*, accordingly.

The molecular formula of compound **7** was deduced as C$_{15}$H$_{24}$O$_4$ from the HRESIMS data. The ^{1}H NMR data of **7** were similar to those of **6** (Table 3). The obvious differences were the appearance of two doublet methyl groups at δ_H 0.97 and 0.83 (Me-12 and 13) and an oxygenated methylene at δ_H 3.65 and 3.55 (H$_{ab}$-14) in **7**. The COSY correlations between Me-12(13)/H-11/H-7/H$_{ab}$-8/H$_{ab}$-9/H-10/H$_{ab}$-14 established the planar structure of **7** as shown. The relative configuration at C-1, C-2, C-6, and C-7 of **7** was the same as that found for **6** based on the similar coupling constants and NOE relationships. In addition, the large coupling constant between H-1 and H-10 (9.9 Hz) and the NOE correlation between H-1/H$_a$-14 and between H-6/H-10 indicated a *β*-orientation of H-10 in **7** as shown.

Table 3. ^{1}H and ^{13}C NMR Data of Compounds 5−7

	5[a]		6[b]		7[a]	
position	δ_C, type	δ_H (J in Hz)	δ_C, type	δ_H (J in Hz)	δ_C, type	δ_H (J in Hz)
1	73.7, CH	3.69, t (2.3)	52.2, CH	1.97, t (10.0)	51.9, CH	1.13, q (9.9)
2			67.6, CH	3.95, td (10.0, 5.7)	72.1, CH	3.76, td (9.9, 5.9)
3	67.1, CH$_2$	4.44, dd (16.5, 1.4)	34.5, CH$_2$	2.80, dd (15.8, 5.7)	35.2, CH$_2$	2.71, m
		4.30, dt (16.5, 2.3)		2.08, dd (15.8, 10.0)		2.16, m
4	130.7, C		127.1, C		129.5, C	
5	143.2, CH	7.22, ddd (6.1, 2.3, 1.4)	144.2, CH	7.85, br s	140.6, CH	7.06, br s
6	40.2, CH	2.01, m	48.5, CH	2.12, m	44.7, CH	1.92, m
7	46.3, CH	1.60, m	53.9, CH	1.64, ddd (12.7, 8.8, 3.5)	47.2, CH	1.21, m
8	25.0, CH$_2$	1.70, m	33.1, CH$_2$	2.02, m	25.3, CH$_2$	1.77, m
		1.12, qd (12.8, 3.2)		1.17, qd (12.7, 4.6)		1.19, m
9	24.6, CH$_2$	1.58, m	38.1, CH$_2$	2.39, ddd (12.7, 4.1, 2.6)	31.8, CH$_2$	1.80, m
		1.30, qd (12.8, 3.2)		2.09, m		1.15, m
10	44.6, CH	1.65, m	149.8, C		46.4, CH	1.42, m
11	28.7, CH	1.92, m	74.2, C		28.4, CH	2.19, m
12	21.7, CH$_3$	0.94, d (7.0)	31.9, CH$_3$	1.23, s	21.7, CH$_3$	0.97, d (6.9)
13	16.3, CH$_3$	0.90, d (6.9)	23.7, CH$_3$	1.18, s	15.3, CH$_3$	0.83, d (6.9)
14	64.7, CH$_2$	3.67, dd (10.7, 7.7)	106.2, CH$_2$	4.94, br s	68.3, CH$_2$	3.63, dd (11.3, 7.0)
		3.47, dd (10.7, 6.1)		4.87, br s		3.55, dd (11.3, 3.4)
15	168.5, C		171.1, C		170.3, C	

[a]Recorded at 600 MHz (^{1}H) and 150 MHz (^{13}C) in CD$_3$OD. [b]Recorded at 300 MHz (^{1}H) and 75 MHz (^{13}C) in CD$_3$OD.
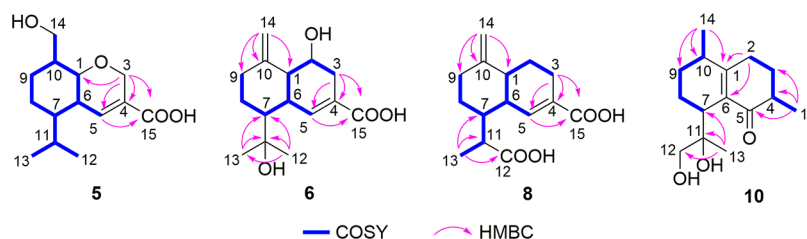
Figure 3. COSY and key HMBC correlations of **5**, **6**, **8**, and **10**.
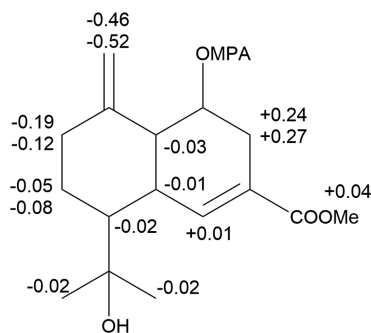
Figure 4. $\Delta\delta^{RS}$ ($\delta_R - \delta_S$) values of (*R*)-MPA ester **6a** and (*S*)-MPA ester **6b**.

Rhinomilisin G (**8**) was obtained as a white, amorphous powder. Based on the HRESIMS data, the molecular formula of **8** was determined to be C$_{15}$H$_{20}$O$_4$. Comparison of the NMR data of **8** (Table 4) and **6** revealed the disappearance of the methyl group (C-12) and the oxygenated methine (C-2) in **8**. The COSY correlations between H-1/H$_{ab}$-2/H$_{ab}$-3 and between H-7/H-11/H-13 as well as the HMBC correlations from Me-13 to C-7 (δ_C 44.0), C-11 (δ_C 40.2), and C-12 (δ_C 179.6) indicated an aliphatic methylene and a carboxylic acid group to be located at C-2 and C-12, respectively (Figure 3). The remaining structure of **8** was identical to that of **6** as determined by detailed analysis of the 2D NMR spectra of **8**. The large values of $^2J_{\text{H-1/Hb-2}}$ (10.9 Hz), $^2J_{\text{H-1/H-6}}$ (10.9 Hz),

$^2J_{\text{H-6/H-7}}$ (12.0 Hz), and $^2J_{\text{H-7/Hb-8}}$ (12.0 Hz), together with the NOE correlations between H$_b$-2/H-6, H-6/H$_b$-8, and H-1/H-7, revealed that H$_b$-2, H-6, and H$_b$-8 were on the β-face of the ring, while H-1 and H-7 were on the α-face (Figure 5). In addition, the configuration at C-11 was deduced from the NOE correlations from H-11 to H-5 and H-7 as well as from Me-13 to H-5, H-6, and H$_b$-8.

The ^{1}H NMR spectrum of **9** was very similar to that of **8**, indicating their structural similarity. The HRESIMS spectrum of **9** gave the molecular formula C$_{15}$H$_{21}$ClO$_5$, containing an additional chlorine atom when compared to **8**. The obvious difference between the NMR data of **9** and **8** (Table 4) was the upfield shift of the methylene group at C-14 in **9** (δ_H 3.64 and 3.47, H$_{ab}$-14). In the HSQC spectrum of **9**, these two methylene protons were assigned to the carbon at δ_C 51.3, which proved the presence of a chlorinated methylene group at C-14. The hydroxy group at C-10 was evident from the HMBC correlation from H$_{ab}$-14 to an oxygenated carbon (δ_C 72.8). The relative configuration at C-1, C-6, C-7, and C-11 of **9** was the same as found for **8** based on the similar NOE relationships. Moreover, the NOE correlations between H-1/H$_a$-2, H$_a$-2/H$_a$-14, H$_a$-2/H$_b$-14, H$_a$-14/H-1, and H$_b$-2/H-6 indicated the β-orientation of OH-10 in **9** as shown.

The molecular formula of compound **10** was determined as C$_{15}$H$_{24}$O$_3$ by HRESIMS. The ^{1}H NMR spectrum of **10** (Table 4) showed one oxygenated methylene group at δ_H 3.48 and 3.41 (H$_{ab}$-12) and three methyl groups at δ_H 1.22 (d, Me-15),

Table 4. ^{1}H and ^{13}C NMR Data of Compounds 8−10

position	8[a] δ_C, type	8[a] δ_H (J in Hz)	9[b] δ_C, type	9[b] δ_H (J in Hz)	10[a] δ_C, type	10[a] δ_H (J in Hz)
1	44.6, CH	1.89, t (10.9)	43.8, CH	1.56, t (10.7)	145.1, C	
2	26.1, CH$_2$	2.08, m	22.2, CH$_2$	1.91, m	27.4, CH$_2$	2.82, dd (16.7, 1.6)
		1,51, qd (10.9, 5.6)		1.41, m		2.34, dd (16.7, 10.3)
3	25.8, CH$_2$	2.51, m	25.7, CH$_2$	2.45, m	44.1, CH$_2$	2.57, m
		2.24, m		2.18, m		1.96, m
4	132.9, C		132.1, C		38.0, CH	2.80, m
5	139.7, CH	7.04, br s	140.3, CH	7.06, br s	182.8, C	
6	46.1, CH	1.82, m	38.1, CH	2.35, m	106.3, C	
7	44.0, CH	2.01, tt (12.0, 3.5)	43.3, CH	1.79, m	44.3, CH	2.13, m
8	29.8, CH$_2$	1.67, m	22.5, CH$_2$	1.73, m	25.5, CH$_2$	1.94, m
		1.36, qd (12.0, 4.0)		1.38, m		1.44, m
9	36.7, CH$_2$	2.41, ddd (13.1, 4.0, 2.8)	35.1, CH$_2$	1.74, m	29.5, CH$_2$	1.93, m
		2.12, m				1.68, m
10	152.6, C		72.8, C		29.9, CH	2.70, m
11	40.2, CH	3.01, qd (7.1, 3.9)	40.1, CH	3.01, m	75.9, C	
12	179.6, C		179.5, C		68.8, CH$_2$	3.48, d (11.2)
						3.41, d (11.2)
13	9.6, CH$_3$	1.02, d (7.1)	9.4, CH$_3$	1.08, d (7.1)	18.7, CH$_3$	1.05, s
14	105.1, CH$_2$	4.73, br s	51.3, CH$_2$	3.64, d (11.0)	18.1, CH$_3$	1.09, d (7.2)
		4.64, br s		3.47, d (11.0)		
15	171.0, C		170.7, C		19.4, CH$_3$	1.22, d (7.1)

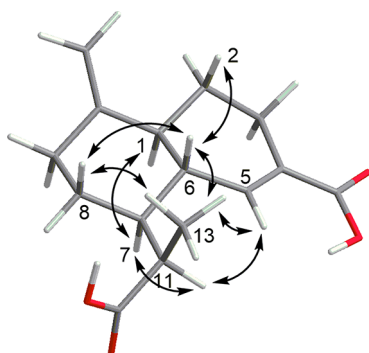[a]Recorded at 600 MHz (^{1}H) and 150 MHz (^{13}C) in CD$_3$OD. [b]Recorded at 700 MHz (^{1}H) and 175 MHz (^{13}C) in CD$_3$OD.

Figure 5. Key NOE correlations of **8**.

1.09 (d, Me-14), and 1.05 (s, Me-13). The COSY correlations established two fragments: C$_2$−C$_3$−C$_4$−C$_{15}$ and C$_7$−C$_8$−C$_9$−C$_{10}$−C$_{14}$ (Figure 3). The 1,2-propandiol-2-yl moiety at C-7 was confirmed by the HMBC correlations from Me-13 to C-7, C-11, and C-12, while the α,β-unsaturated carbonyl group (C$_1$=C$_6$−C$_5$=O) was deduced from the HMBC correlations from Me-14 to C-1, C-9, and C-10, from H$_{ab}$-2 to C-1 and C-6, and from Me-15 to C-3, C-4, and C-5. Thus, the planar structure of **10** was elucidated as shown. Due to the limited amount of sample isolated, no reliable NOE data could be recorded. Thus, the relative configuration of compound **10** was not elucidated.

Previous feeding experiments with ^{13}C-labeled acetate by Stipanovic et al. in 1982 revealed that farnesyl pyrophosphate is the probable precursor to heptelidic acid.[18] It was also suggested that the lactone ring was formed through an enzymatically catalyzed oxygen insertion between C-2 and C-3 from cadalene-type sesquiterpenes (Figure 6).[18] This assumption is further supported by this study since both cadalene-type sesquiterpenes (**6**−**10**) and heptelidic acid derivatives (**1**−**5** and **11**−**16**) were isolated from the same fungal strain. The

compounds with a chloromethyl group (**1**, **2**, **3**, **9**, and **11**) were probably formed by SAM:Cl$^-$ methyltransferase, which is a common halogenase in fungi.[19] The origin of the chlorine substituents is probably from sea salt (3.5 g/flask), which was added to the rice medium in this study with the purpose of mimicking the high-saline environment of the host plant. To prove that **2** was not an artificial product from **11** originating during workup, 1 mg of **11** was kept in 1 mL of 70% MeOH−H$_2$O containing 0.1% trifluoroacetic acid (TFA) for 24 h followed by analysis with TLC. No transformation from **11** to **2** was detected.

All isolated compounds (**1**−**16**) were examined for their cytotoxicity against the mouse lymphoma cell line L5178Y and for their antibacterial activities against *Mycobacterium tuberculosis*, *Enterococcus faecium*, *Staphylococcus aureus*, *Klebsiella pneumoniae*, *Enterobacter aerogenes*, *Escherichia coli*, and *Acinetobacter baumannii*. Compounds **1**, **7**, and **15** showed cytotoxicity with IC$_{50}$ values of 5.0, 8.7, and 24.4 μM, respectively, while only compound **11** showed weak inhibition against *S. aureus* and *E. faecium*, with minimal inhibitory concentration (MIC) values of 50 μM, and against *K. pneumoniae*, with a MIC value of 100 μM.

■ EXPERIMENTAL SECTION

General Experimental Procedures. A P-1020 polarimeter (JASCO, Tokyo, Japan) was used to measure optical rotations. A UHR-QTOF maxis 4G mass spectrometer (Bruker Daltonics) was used to record HRESIMS data. NMR spectra were recorded on Bruker Avance III 300 or 600 spectrometers. A Dionex P580 system containing a photodiode array detector (UVD340s) and a separation column (125 × 4 mm, 5 μm, Eurospher C$_{18}$) was applied for HPLC analysis. A semipreparative HPLC Lachrom-Merck Hitachi system, which contained an L7100 pump, an L7400 UV detector, and a separation column (300 × 8 mm, 10 μm, Eurospher C$_{18}$), was used for HPLC separation. Sephadex LH-20 or MN silica gel 60 M (Merck) was employed for column chromatography. Precoated silica
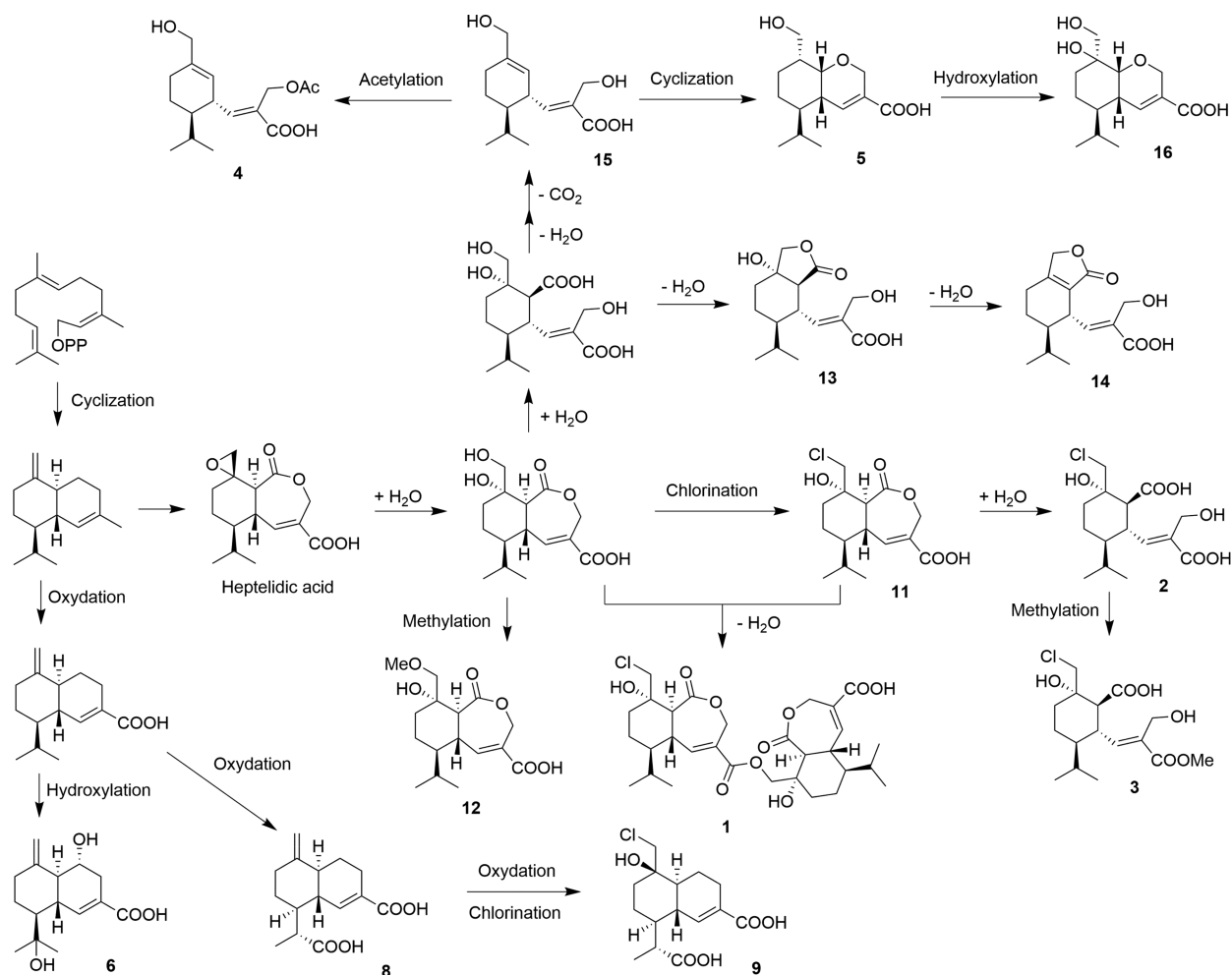
Figure 6. Plausible biogenetic relationship of isolated compounds.

gel 60 F_{254} plates (Merck) were used for thin-layer chromatography (TLC) with detection under 254 and 365 nm.

Fungal Material. The endophytic fungus was isolated from fresh leaves of *Acrostichums aureum* (Pteridaceae), a mangrove fern collected in October 2014 from Douala in Cameroon. The plant was identified by one of the authors (S.H.A.), and a voucher specimen (No. 20141004-C-7-BL) was deposited in the lab of P.P. Leaves of the plant were washed twice with sterile water, and after drying, the surface was sterilized by 70% ethanol for 1 min in a laminar flow hood. After drying, the leaves were cut into small pieces (1 × 1 × 1 cm) and transferred on the fungal isolation medium (0.2 g/L chloramphenicol, 15 g/L agar, and 15 g/L malt extract in distilled water, pH 7.4−7.8), then incubated for several days at 20 °C. During the fungal purification, Czapek's agar medium was also used to facilitate the growth of hyphae. After purification, the fungus was inoculated on solid rice medium in an Erlenmeyer flask (1 L) for cultivation. The fungus was identified as *Rhinocladiella similis* (GenBank accession number KX363812) according to the molecular biological protocol as described previously.[20] The fungal strain (No. C-7-BL-2) was kept in the lab of P.P.

Fermentation, Extraction, and Isolation. Ten 1 L Erlenmeyer flasks with solid rice medium containing sea salt (100 g of rice, 3.5 g of sea salt, 3.0 g of sucrose, and 110 mL of demineralized water) were employed for fermentation. After autoclaving (121 °C, 20 min) the medium, the fungal colonies were inoculated onto the medium. After 77 days of cultivation at 20 °C under static conditions, the hyphae finally reached the bottom of the medium. The fermentation was terminated by adding 500 mL of EtOAc to each flask. The flasks were shaken at 150 rpm for 8 h. Then the EtOAc solution was evaporated to dryness.

The obtained brown extract (7.5 g) was subjected to silica gel vacuum liquid chromatography using solvents (500 mL each gradient) in a gradient of increasing polarity (*n*-hexane−EtOAc, 9:1, 7:3, 1:1; dichloromethane−methanol, 15:1, 6:1, 0:1) to yield 11 fractions. Fr. E (192 mg) was subjected to a Sephadex LH-20 column using 100% MeOH as mobile phase to remove pigments, followed by purification with semipreparative HPLC [methanol in H_2O (with 0.1% TFA): 0−5 min, 35%; 5−15 min, from 35% to 58%; 16−19 min, 100%] to yield **2** (52.7 mg) and **8** (7.7 mg). Following similar procedures, Fr. F (440 mg) yielded **3** (15.3 mg) [HPLC sequence, methanol in H_2O (with 0.1% TFA): 0−10 min, from 35% to 45%; 10−25 min, from 45% to 60%; 26−30 min, 100%], Fr. G (200 mg) afforded **11** (161.2 mg) [HPLC sequence, methanol in H_2O (with 0.1% TFA): 0−10 min, from 30% to 40%; 10−20 min, from 40% to 60%; 22−26 min, 100%], while Fr. H (1400 mg) afforded **1** (3.5 mg), **4** (1.3 mg), **5** (3.2 mg), **6** (14.7 mg), **7** (6.4 mg), **9** (1.8 mg), **10** (0.8 mg), **12** (14.9 mg), **13** (29.2 mg), **14** (9.0 mg), **15** (2.1 mg), and **16** (5.4 mg) [HPLC sequence, methanol in H_2O (with 0.1% TFA): 0−10 min, from 20% to 35%; 10−30 min, from 35% to 70%; 32−36 min, 100%].

Rhinomilisin A (1): white, amorphous powder; $[\alpha]^{20}_D$ −12 (*c* 0.7, MeOH); UV (MeOH) λ_{max} (log ε) 219 (4.35); ^1H and ^{13}C NMR data, see Table 1; HRESIMS *m/z* 614.2724 $[M + NH_4]^+$ (calcd for $C_{30}H_{45}ClNO_{10}$, 614.2727).

Rhinomilisin B (2): white, amorphous powder; $[\alpha]^{20}_D$ +41 (*c* 3.0, MeOH); UV (MeOH) λ_{max} (log ε) 219 (4.23); ^1H and ^{13}C NMR data, see Table 2; HRESIMS *m/z* 335.1255 $[M + H]^+$ (calcd for $C_{15}H_{24}ClO_6$, 335.1256), 352.1522 $[M + NH_4]^+$ (calcd for $C_{15}H_{27}ClNO_6$, 352.1521).

Rhinomilisin C (3): colorless crystals; $[\alpha]^{20}_D$ +37 (*c* 1.5, MeOH); UV (MeOH) λ_{max} (log ε) 218 (4.34); ^{1}H and ^{13}C NMR data, see Table 2; HRESIMS *m/z* 349.1413 [M + H]$^+$ (calcd for $C_{16}H_{26}ClO_6$, 349.1412), 366.1682 [M + NH$_4$]$^+$ (calcd for $C_{16}H_{29}ClNO_6$, 366.1678).

Rhinomilisin D (4): colorless oil; $[\alpha]^{20}_D$ +73 (*c* 0.2, MeOH); UV (MeOH) λ_{max} (log ε) 218 (4.12); ^{1}H and ^{13}C NMR data, see Table 2; HRESIMS *m/z* 297.1693 [M + H]$^+$ (calcd for $C_{16}H_{25}O_5$, 297.1697), 319.1512 [M + Na]$^+$ (calcd for $C_{16}H_{24}O_5Na$, 319.1516).

Rhinomilisin E (5): colorless oil; $[\alpha]^{20}_D$ +5 (*c* 0.8, MeOH); UV (MeOH) λ_{max} (log ε) 218 (3.68); ^{1}H and ^{13}C NMR data, see Table 3; HRESIMS *m/z* 255.15891 [M + H]$^+$ (calcd for $C_{14}H_{23}O_4$, 255.1591), 277.1409 [M + Na]$^+$ (calcd for $C_{14}H_{22}O_4Na$, 277.1410).

Rhinomilisin F (6): white, amorphous powder; $[\alpha]^{20}_D$ −93 (*c* 1.2, MeOH); UV (MeOH) λ_{max} (log ε) 218 (3.67), 233 (3.72); ^{1}H and ^{13}C NMR data, see Table 3; HRESIMS *m/z* 284.1854 [M + NH$_4$]$^+$ (calcd for $C_{15}H_{26}NO_4$, 284.1856), 289.1408 [M + Na]$^+$ (calcd for $C_{15}H_{22}O_4Na$, 289.1410).

Rhinomilisin G (7): colorless oil; $[\alpha]^{20}_D$ −51 (*c* 0.9, MeOH); UV (MeOH) λ_{max} (log ε) 220 (3.70); ^{1}H and ^{13}C NMR data, see Table 3; HRESIMS *m/z* 269.1746 [M + H]$^+$ (calcd for $C_{15}H_{25}O_4$, 269.1747), 291.1563 [M + Na]$^+$ (calcd for $C_{15}H_{24}O_4Na$, 291.1567).

Rhinomilisin H (8): white, amorphous powder; $[\alpha]^{20}_D$ −89 (*c* 1.0, MeOH); UV (MeOH) λ_{max} (log ε) 218 (3.69), 234 (3.73); ^{1}H and ^{13}C NMR data, see Table 4; HRESIMS *m/z* 282.1701 [M + NH$_4$]$^+$ (calcd for $C_{15}H_{24}NO_4$, 282.1700), 287.1254 [M + Na]$^+$ (calcd for $C_{15}H_{20}O_4Na$, 287.1254).

Rhinomilisin I (9): colorless oil; $[\alpha]^{20}_D$ −8 (*c* 0.3, MeOH); UV (MeOH) λ_{max} (log ε) 219 (3.71); ^{1}H and ^{13}C NMR data, see Table 4; HRESIMS *m/z* 334.1417 [M + NH$_4$]$^+$ (calcd for $C_{15}H_{25}ClNO_5$, 334.1416).

Rhinomilisin J (10): colorless oil; $[\alpha]^{20}_D$ +1 (*c* 0.2, MeOH); UV (MeOH) λ_{max} (log ε) 244 (4.24); ^{1}H and ^{13}C NMR data, see Table 4; HRESIMS *m/z* 253.1800 [M + H]$^+$ (calcd for $C_{15}H_{25}O_3$, 253.1798).

X-ray Crystallographic Analysis of Rhinomilisin C (3). Compound **3** as the 1.5H$_2$O hydrate was measured with a Bruker Kappa APEX2 CCD diffractometer with a microfocus tube, Mo Kα radiation (λ = 1.541 78 Å). APEX2 was used for data collection, SAINT was used for cell refinement and data reduction,[21] and SADABS was used for experimental absorption correction.[22] The structure was solved by intrinsic phasing using SHELXT,[23] while refinement was done by full-matrix least-squares on F^2 using SHELXL-2014/7.[24] The hydrogen atoms were positioned geometrically (with C−H = 0.95 Å for aromatic CH, 1.00 Å for aliphatic CH, 0.99 Å for CH$_2$, and 0.98 Å for CH$_3$) and refined using riding models (AFIX 43, 13, 23, 137, respectively), with $U_{iso}(H) = 1.2U_{eq}(CH, CH_2)$ and $1.5U_{eq}(CH_3)$. The hydrogen atoms in the hydroxy groups and water molecules were found and freely refined with $U_{iso}(H) = 1.5U_{eq}(O)$. The absolute configuration of **3** was solved using anomalous dispersion from Mo Kα, resulting in a Flack parameter of 0.040(15) using Parsons' quotient method.[25] Graphics were drawn using DIAMOND.[26] The structural data have been deposited in the Cambridge Crystallographic Data Center (CCDC No. 1869183).

Crystal data of 3: $2(C_{16}H_{25}ClO_6)\cdot3(H_2O)$, M = 751.66, monoclinic system, space group *C*2, *a* = 18.0154(15) Å, *b* = 6.3425(5) Å, *c* = 16.3801(13) Å, *V* = 1817.5(3) Å^3, Z = 2, D_{calc} = 1.373 g/cm^3, crystal size 0.70 × 0.30 × 0.20 mm^3, μ(Mo Kα) = 0.247 mm^{-1}, 2.3° < θ < 25.5°, N_t = 7316, N = 3134 (R_{int} = 0.0136), R_1 = 0.0260, wR_2 = 0.0654, S = 1.111, Flack parameter 0.040(15).

Preparation of (*R*)- and (*S*)-MPA Esters of Compound 6. Compound **6** (5 mg) was dried overnight using a freeze-dryer and then dissolved in 500 μL of dimethylformamide in a 5 mL flask. Then 1.0 mg of dry K$_2$CO$_3$ was added, and after stirring for 2 h, 5 μL of MeI was added. After stirring at room temperature for 24 h, the mixture was poured into 2 mL of water and then extracted with 2 mL of EtOAc three times. The EtOAc phase was further dried to afford 2 mg of methylated product of compound **6**, which was then divided to two 5 mL flasks followed by addition of 500 μL of dichloromethane, 0.5 mg of dimethylaminopyridine, 3.4 mg of dicyclohexylcarbodiimide, and 6 mg of (*R*)- or (*S*)-α-methoxy-α-phenylacetic acid (MPA). After

stirring for 24 h at room temperature, the two reaction mixtures were filtered, dried, and further purified by semipreparative HPLC using 70% acetonitrile as mobile phase to give 0.7 mg of pure (*R*)- and (*S*)-MPA esters **6a** and **6b**, respectively.

(R)-MPA ester 6a: ^{1}H NMR (CD$_3$OD, 600 MHz) δ 7.39−7.32 (5H, m, phenyl protons of MPA), 7.88 (1H, br s, H-5), 5.12 (1H, ddd, *J* = 11.1, 9.4, 6.1 Hz, H-2), 4.81 (1H, s, CH of MPA), 4.26 (1H, br s, H$_a$-14), 3.88 (1H, br s, H$_b$-14), 3.71 (3H, s, COOMe), 3.39 (3H, s, OMe of MPA), 2.93 (1H, m, H$_a$-3), 2.22 (1H, dd, *J* = 11.1, 10.5 Hz, H-1), 2.19 (1H, m, H$_a$-9), 2.17 (1H, m, H-6), 2.13 (1H, m, H$_b$-3), 1.98 (1H, m, H$_b$-9), 1.97 (1H, m, H$_a$-8), 1.63 (1H, m, H-7), 1.21 (3H, s, Me-12), 1.15 (3H, s, Me-13), 1.09 (1H, m, H$_b$-8).

(S)-MPA ester 6b: ^{1}H NMR (CD$_3$OD, 600 MHz) δ 7.42−7.34 (5H, m, phenyl protons of MPA), 7.87 (1H, br s, H-5), 5.22 (1H, ddd, *J* = 11.0, 9.5, 6.1 Hz, H-2), 4.80 (1H, s, CH of MPA), 4.72 (1H, br s, H$_a$-14), 4.40 (1H, br s, H$_b$-14), 3.67 (3H, s, COOMe), 3.38 (3H, s, OMe of MPA), 2.69 (1H, m, H$_a$-3), 2.38 (1H, m, H$_a$-9), 2.25 (1H, dd, *J* = 11.0, 10.6 Hz, H-1), 2.18 (1H, m, H-6), 2.10 (1H, m, H$_b$-9), 2.02 (1H, m, H$_a$-8), 1.86 (1H, m, H$_b$-3), 1.65 (1H, m, H-7), 1.23 (3H, s, Me-12), 1.17 (3H, s, Me-13), 1.17 (1H, m, H$_b$-8).

Cytotoxicity Assay. Cytotoxicity was tested against the mouse lymphoma cell line L5178Y using a microplate 3-(4,5-dimethylthiazole-2-yl)-2,5-diphenyltetrazolium bromide (MTT) assay as described before.[27] Experiments were repeated three times. Kahalalide F (IC$_{50}$ 4.3 μM) obtained from *Elysia grandifolia* was used as positive control, while media with 0.1% ethylene glycol monomethyl ether (EGMME)−DMSO were included as negative control.

Antibacterial Assay. Antibacterial activities were evaluated by calculating MIC values against *M. tuberculosis*, *E. faecium* ATCC35667, *S. aureus* ATCC29213, *K. pneumoniae* ATCC13883, *E. aerogenes* ATCC13048, *E. coli* ATCC25922, and *A. baumannii* ATCCBAA1605 using the broth microdilution method according to CLSI guidelines.[28] Moxifloxacin and rifampicin were used as positive controls against the Gram-positive and Gram-negative bacteria, respectively.

■ ASSOCIATED CONTENT

Ⓢ Supporting Information

The Supporting Information is available free of charge on the ACS Publications website at DOI: 10.1021/acs.jnatprod.8b00938.

> HRESIMS, UV, and NMR spectra of compounds **1**−**10** (PDF)
>
> X-ray crystallographic data (CIF)

■ AUTHOR INFORMATION

Corresponding Authors

*Tel: +49 211 81 15979. Fax: +49 211 81 11923. E-mail: zhenfeizi0@sina.com (Z.L.).

*Tel: +49 211 81 14163. Fax: +49 211 81 11923. E-mail: proksch@uni-duesseldorf.de (P.P.).

ORCID

Christoph Janiak: 0000-0002-6288-9605

Zhen Liu: 0000-0003-3314-7853

Notes

The authors declare no competing financial interest.

■ REFERENCES

(1) Beekman, A. M.; Barrow, R. A. *Aust. J. Chem.* **2014**, *67*, 827−843.

(2) Xu, J. *RSC Adv.* **2015**, *5*, 841−892.

(3) Rateb, M. E.; Ebel, R. *Nat. Prod. Rep.* **2011**, *28*, 290−344.

(4) Singh, A. V.; Bandi, M.; Raje, N.; Richardson, P.; Palladino, M. A.; Chauhan, D.; Anderson, K. C. *Blood* **2011**, *26*, 5692−5700.

(5) Gomes, N. G. M.; Lefranc, F.; Kijjoa, A.; Kiss, R. *Mar. Drugs* **2015**, *13*, 3950−3991.

(6) Liu, S.; Dai, H.; Orfali, R. S.; Lin, W.; Liu, Z.; Proksch, P. *J. Agric. Food Chem.* **2016**, *64*, 3127−3132.

(7) Liu, S.; Dai, H.; Makhloufi, G.; Heering, C.; Janiak, C.; Hartmann, R.; Mándi, A.; Kurtán, T.; Müller, W. E. G.; Kassack, M.; Lin, W.; Liu, Z.; Proksch, P. *J. Nat. Prod.* **2016**, *79*, 2332−2340.

(8) Wang, H.; Eze, P. M.; Höfert, S.-P.; Janiak, C.; Hartmann, R.; Okoye, F. B. C.; Esimone, C. O.; Orfali, R. S.; Dai, H.; Liu, Z.; Proksch, P. *RSC Adv.* **2018**, *8*, 7863−7872.

(9) Yan, S.; Li, S.; Wu, W.; Zhao, F.; Bao, L.; Ding, R.; Gao, H.; Wen, H.-A.; Song, F.; Liu, H.-W. *Chem. Biodiversity* **2011**, *8*, 1689−1700.

(10) Yamaguchi, Y.; Manita, D.; Takeuchi, T.; Kuramochi, K.; Kuriyama, I.; Sugawara, F.; Yoshida, H.; Mizushina, Y. *Biosci., Biotechnol., Biochem.* **2010**, *74*, 793−801.

(11) Calhoun, L. A.; Findlay, J. A.; Miller, J. D.; Whitney, N. J. *Mycol. Res.* **1992**, *96*, 281−286.

(12) Itoh, Y.; Takahashi, S.; Arai, M. *J. Antibiot.* **1982**, *4*, 541−542.

(13) Rahier, N. J.; Molinier, N.; Long, C.; Deshmukh, S. K.; Kate, A. S.; Ranadive, P.; Verekar, S. A.; Jiotode, M.; Lavhale, R. R.; Tokdar, P.; Balakrishnan, A.; Meignan, S.; Robichon, C.; Gomes, B.; Aussagues, Y.; Samson, A.; Sautel, F.; Bailly, C. *Bioorg. Med. Chem.* **2015**, *23*, 3712−3721.

(14) Kato, M.; Sakai, K.; Endo, A. *Biochim. Biophys. Acta, Protein Struct. Mol. Enzymol.* **1992**, *1120*, 113−116.

(15) Kim, J. H.; Lee, C. H. *J. Microbiol. Biotechnol.* **2009**, *19*, 787−791.

(16) Wei, H.; Xu, Y.; Espinosa-Artiles, P.; Liu, M. X.; Luo, J.-G.; U'Ren, J. M.; Arnold, A. E.; Gunatilaka, A. A. L. *Phytochemistry* **2015**, *118*, 102−108.

(17) Kawashima, J.; Ito, F.; Kato, T.; Niwano, M.; Koshino, H.; Uramoto, M. *J. Antibiot.* **1994**, *47*, 1562−1563.

(18) Stipanovic, R. D.; Howell, C. R. *Tetrahedron* **1983**, *39*, 1103−1107.

(19) Brakhage, A. A.; Shroeckh, V. *Fungal Genet. Biol.* **2011**, *48*, 15−22.

(20) Kjer, J.; Debbab, A.; Aly, A. H.; Proksch, P. *Nat. Protoc.* **2010**, *5*, 479−490.

(21) *Apex2*, Data Collection Program for the CCD Area-Detector System; *SAINT*, Data Reduction and Frame Integration Program for the CCD Area-Detector System; Bruker Analytical X-ray Systems: Madison, WI, USA, 1997−2012.

(22) Sheldrick, G. M. *SADABS: Area-detector absorption correction*; University of Göttingen: Germany, 1996.

(23) Sheldrick, G. M. *Acta Crystallogr., Sect. A: Found. Crystallogr.* **2008**, *64*, 112−122.

(24) Sheldrick, G. M. *Acta Crystallogr., Sect. C: Struct. Chem.* **2015**, *71*, 3−8.

(25) Parsons, S.; Flack, H. D.; Wagner, T. *Acta Crystallogr., Sect. B: Struct. Sci., Cryst. Eng. Mater.* **2013**, *69*, 249−259.

(26) Brandenburg, K. *Diamond* (Version 4.2), Crystal and Molecular Structure Visualization, Crystal Impact − K; Brandenburg & H. Putz Gbr: Bonn, Germany, 2018.

(27) Ashour, M.; Edrada, R.; Ebel, R.; Wray, V.; Wätjen, W.; Padmakumar, K.; Müller, W. E. G.; Lin, W. H.; Proksch, P. *J. Nat. Prod.* **2006**, *69*, 1547−1553.

(28) CLSI. *Methods for Dilution Antimicrobial Susceptibility Tests for Bacteria That Grow Aerobically*; Approved Standard, ninth ed.; Clinical and Laboratory Standards Institute, 2012.